Coupled Translations of the 64-Meter Antenna Subreflector Supports

M. S. Katow
Ground Antenna and Facilities Engineering Section

The Tricone subreflector assembly of the 64-m diameter antenna is supported from the apex of the quadripod by six flexure rods. The subreflector can be translated in the three orthogonal axes by jackscrews at the ends of each rod. The arrangement of the six rods is described and analysis of the position errors introduced by coupled translations is presented. The results indicate that negligible RF gain losses caused by axis-coupled translations (less than 0.05 dB) are possible at X-band (8.45 GHz) operation.

I. Introduction

The existing subreflector of the 64-m antenna, employing the Tricone RF feed system, is supported from the quadripod apex by six rods, each with flexures at both ends as shown in Figs. 1 and 2. A jackscrew is located at one end of each rod. Three rods are used for the A-axis motion, two rods for the Y-axis motion and one rod for the X-axis motion. The subreflector can be translated in the three orthogonal directions X, Y and Z by changes in the lengths of these rods by motorized jackscrews using worm gears. The RF feed cone-to-RF feed cone rotation of the subreflector is provided by a rotational drive mechanism.

In the Tricone RF feed system, the sloped axis of the subreflector is rotated about the symmetric axis of the reflector to one of the three main RF feed positions A, B or C (Fig. 3).

Because the reflective surfaces (the main reflector and the subreflector) are rigged or set at 45 degrees elevation angle, the rotation of the antenna to other elevation angles introduces more gravity loading distortions that result in RF phase center offsets at the paraboloid's prime focus, which in turn produce RF gain losses. Accordingly, the subreflector can be translated with respect to its supporting quadripod by length changes of the supporting rods to minimize these offsets and reduce the antenna's resulting RF gain losses.

The arrangement of the six supporting rods results in a statically determinate type truss where a small length change of any rod produces a minimal change in the axial force. The use of flexures has minimized any moments or bending stresses in the rods.

The geometrical arrangement of the subreflector support rods is described in this article together with the analysis and computation of the cross couplings of the corrective translations and the resulting gain losses. The goal was to estimate how much the gain losses can be caused by these axis-coupling position errors.

II. Analysis

The coordinate system of the supporting rods was chosen parallel to the symmetric axis of the main reflector with the

angular difference of 4 deg and 31 min between the axis of the main reflector and the subreflector axis. In the isometric view of Fig. 4, the angles between the hyperboloid axis and the two planes parallel to the symmetric axis of the main reflector for the subreflector in position A are shown.

The subreflector is supported in the axial-Z direction by three flexure rods as shown in Figs. 1 and 2. These rods also constrain the rotational moments about the X and Y axes to account for three degrees of freedom. Three jackscrews driven in unison control the Z-axis translation.

In the lateral-Y direction, two rods driven in unison are used to account for the rotation constraint about the Z-axis as well as the Y translation. These two rods account for two more degrees of freedom.

By arranging the design to connect the sliding anchor on the subreflector end of the X-lateral constraint to the end of a Y-lateral strut, as shown in Fig. 1, it was possible to eliminate the axis-coupled translations in the X-direction resulting from the large Y-lateral corrections. The gain loss due to the induced azimuth pointing (or boresight) error would not have satisfied operational requirements without correction. The X-lateral constraint adds to the six degrees required for stability.

Starting with the subreflector aligned with the main reflector's symmetric axis at the 45 deg elevation angle, raising the 64-m antenna to 84 deg elevation generates 7.62 cm (3.0 in.) lateral offset between the focus of the best fit paraboloid of the main reflector and the deflected virtual focus of the subreflector system. This lateral Y defocus can be continuously corrected by jackscrews adjusting the lengths of the Y lateral rods through the change in the elevation angles. The cross-coupled axial Z defocus resulting from the lateral Y corrections is described in Fig. 5 and defined in Table 1.

During the elevation angle change, axial Z defocus also occurs. From the set 45-deg position, an axial Z defocus of +0.76 cm occurs close to 80-deg elevation angle and of −2.03 cm at 10-deg elevation angle, as changes from the 45-deg elevation angle.

When the axial Z defocus is corrected by the jackscrews on the Z axial rods, four coupled sources of gain losses are generated. Figure 6 shows the lateral cross-coupled defocus in the Y-direction (view-AA) and in the X direction (view-BB) defining two of the sources of gain losses with calculated lateral offsets in Table 2. The third lateral offset occurs because the axis of the subreflector is tilted 4 deg and 31 min to the axial Z motion. Figure 7 describes the lateral offsets from this source with the numerical offsets shown in Table 3.

The vector sum of the lateral offsets of Tables 2 and 3 are added and shown in Table 4 for the three basic RF feed cone positions only for the maximum −2.03 cm Z focus position.

The subreflector's lateral offsets can be redefined as the offsets of the vertex, and the lateral defocus of Fig. 9 can be calculated. This defocus results in a gain loss as calculated in Fig. 8. The gain loss calculations of Fig. 8 are described in Ref. 1. Additional gain loss occurs due to boresight errors as shown in Fig. 9. This loss should be added to the gain loss described in Table 4.

III. Summary

The existing six supporting rods of the subreflector assembly generate axis-coupled translations which, when combined with the translations required to correct the phase centers offsets, result in less than 0.05 dB RF gain loss at X-band (8.45 GHz).

For a higher RF frequency operation the corrective translations will be significant and should be added to the new microprocessor now used to control the subreflector. New subreflector rotations about the X and Y axes can also be superimposed, if required later on, by adding differential gear boxes to the shafts between the jackscrews driving the three Z-axis supporting rods.

Reference

1. Katow, M. S. "34-Meter Antenna-Subreflector Translations to Maximize RF Gain," *TDA Progress Report 42–62*, Jan. and Feb. 1981, pp. 112–120.

Table 1. Gain loss from *Z*-axis defocus resulting from lateral-*Y* motion (see Fig. 5, cone positions *A*, *B*, or *C*)

Sequence	*Y*-Offset (YOF), cm (in.)	Angle (α), deg[a]	*A*, cm (in.)[b]	*B* Defocus, cm (in.)[c]	Gain Loss, dB[d]
1	2.54 (1.00)	0.4668	311.78 (122.748)	0.01 (0.004)	<0.0001
2	5.08 (2.00)	0.9336	311.75 (122.736)	0.04 (0.016)	0.0004
3	7.62 (3.00)	1.4004	311.70 (122.715)	0.09 (0.035)	0.0023
4	10.16 (4.00)	1.8674	311.62 (122.687)	0.17 (0.067)	0.0079

[a] $\alpha = \sin -1\ (YOF/311.79)$

[b] $A = \sqrt{(311.79)^2 + (YOF)^2}$

[c] $B = 311.79 - A$

[d] See Fig. 8

Table 2. Lateral *X* (Fig. 6, view BB) or *Y* (Fig. 6, view AA) travel cross-coupled to $\pm Z$ axial focus motion for cone positions *A*, *B*, or *C*

Axial-*Z* Focus Motion, cm (in.)	*H*, cm (in.)[a]	*I*, cm (in.)[b]	*J*, cm (in.)[c]	*K*, cm (in.)[d]
+0.76 (+0.3)	253.371 (99.752)	+0.0010 (+0.0004)	251.4589 (99.000)	+0.0011 (+0.0004)
−2.03 (−0.8)	253.362 (99.749)	+0.0080 (+0.0032)	251.4518 (98.9968)	+0.0082 (+0.0032)

[a] $H = \sqrt{253.370^2 - Z^2}$

[b] $I = 253.370 - H$

[c] $J = \sqrt{251.460^2 - Z^2}$

[d] $K = 251.460 - I$

Table 3. Lateral *X* and *Y* offsets for ±*Z* axial focus motions. Angular offset to subreflector axis is 4 deg. 31 min. (See Fig. 7 for lateral *Y* offset and lateral *X* offset.)

Cone Position	*A*, *B*	*A*	*B*	*C*
Axial-*Z* Focus Motion, cm (in.)	*L*, cm (in.)[a]	*M*, cm (in.)[b]	*N*, cm (in.)[c]	*P*, cm (in.)[d]
+0.76 (+0.3)	0.030 (0.012)	−0.052 (−0.020)	0.052 (0.020)	0.060 (0.236)
−2.03 (−0.8)	−0.080 (0.031)	0.139 (0.055)	−0.139 (−0.055)	0.060 (−0.063)

[a] $L = 0.76 \tan(2.2566)$; $L = 2.03 \tan(2.2566)$
[b] $M = 0.76 \tan(3.9106)$; $M = 2.03 \tan(3.9106)$
[c] $N = 0.76 \tan(3.9106)$; $N = 2.03 \tan(3.9106)$
[d] $P = 0.76 \tan(4.5167)$; $P = 2.03 \tan(4.5167)$

Table 4. X-band (8.45 GHz) gain loss from cross-coupled lateral and boresight error for −2.03 cm *Z* focus (see Figs. 7 and 9)

Parameter	Cone Position		
	A	*B*	*C*
Lateral-*Y* Travel, cm	$I = +0.008$	$I = +0.001$	$I = +0.001$
Lateral-*X* Travel, cm	$K = +0.008$	$K = +0.008$	$K = +0.008$
Lateral-*Y* Offset, cm	$L = -0.080$	$L = -0.080$	$P = -0.160$
Lateral-*X* Offset, cm	$M = 0.139$	$N = -0.139$	0
Subreflector Vertex Vector Sum Offset, cm	0.164	0.153	0.159
Lateral Defocus, cm	0.130	0.122	0.126
Lateral Defocus Gain Loss, dB	−0.00022	−0.00019	−0.00021
Boresight Error, deg	0.0023	0.0022	0.0023
Boresight Error Gain Loss, dB	−0.049	−0.045	−0.049
Total Gain Loss, dB	−0.0492	−0.0452	−0.0491

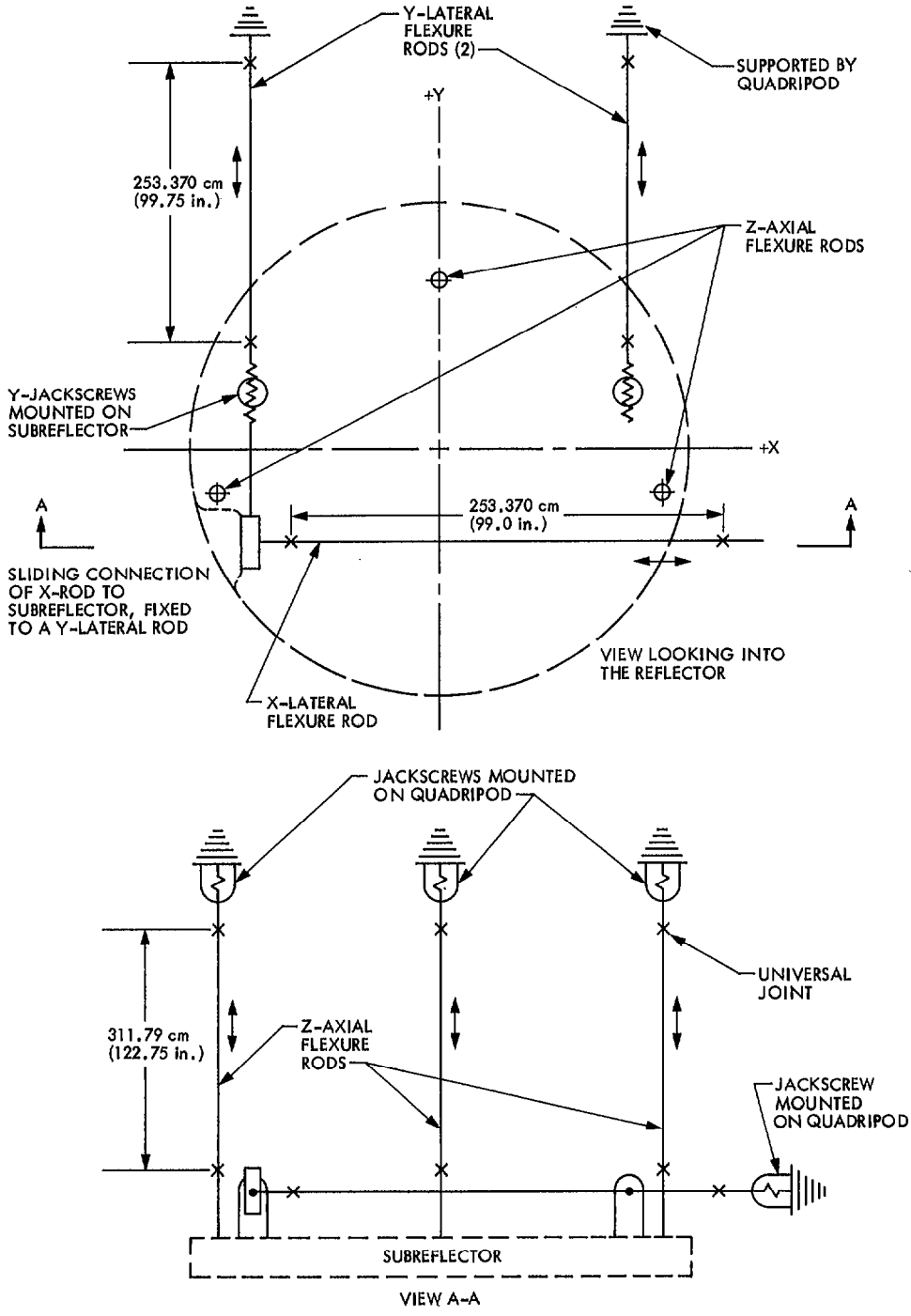

Fig. 1. Flexure supports for the 64-m antenna subreflector

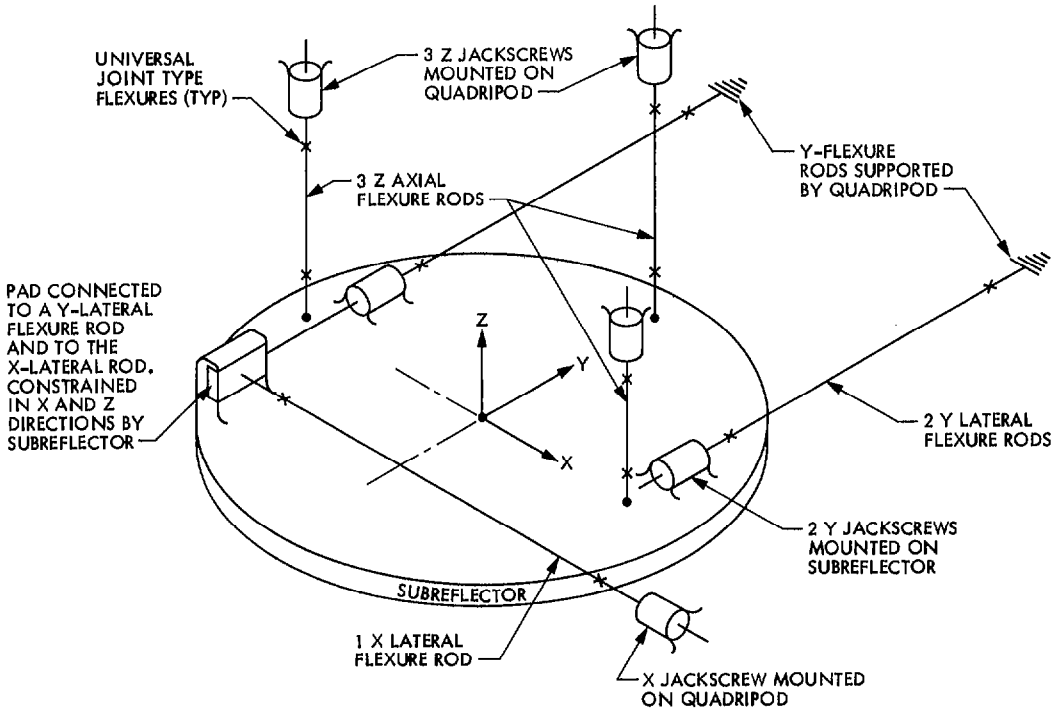

Fig. 2. Isometric view of the 64-m subreflector supports

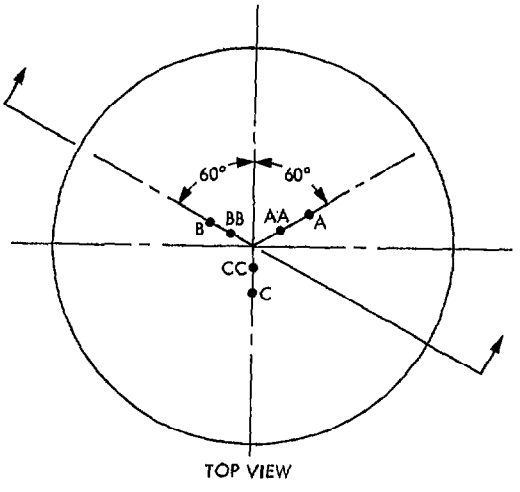

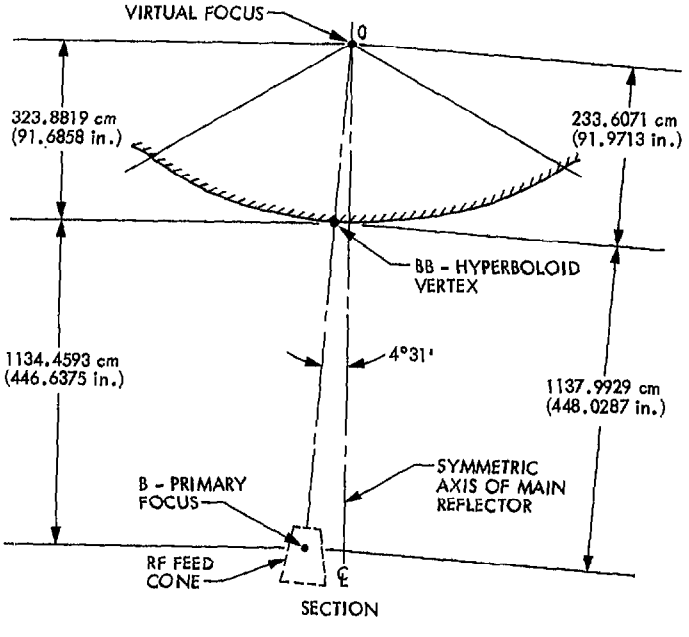

Fig. 3. The 64-m Tricone subreflector geometry

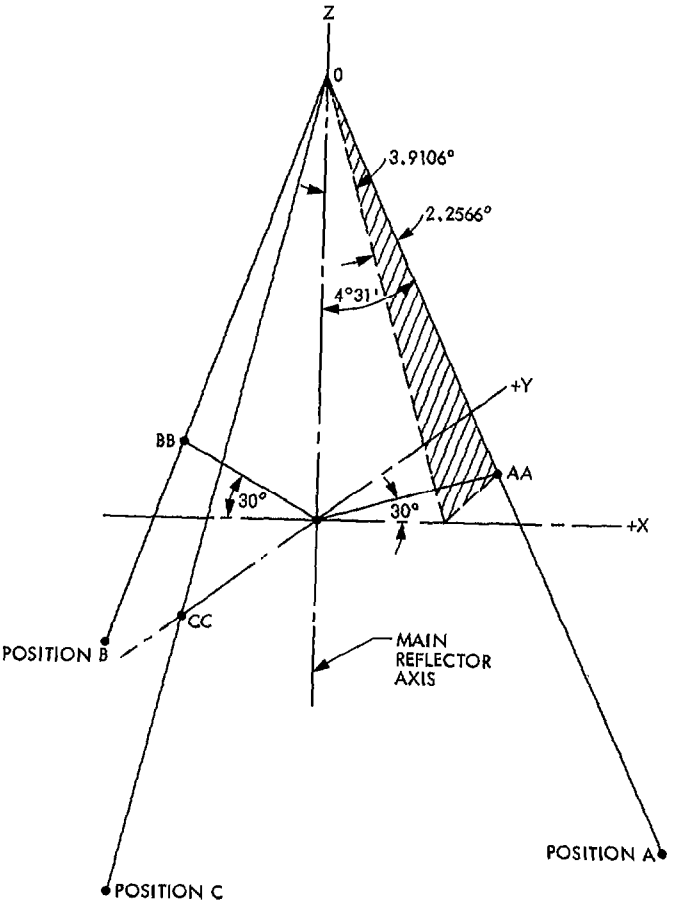

Fig. 4. The 64-m subreflector axis orientation positions

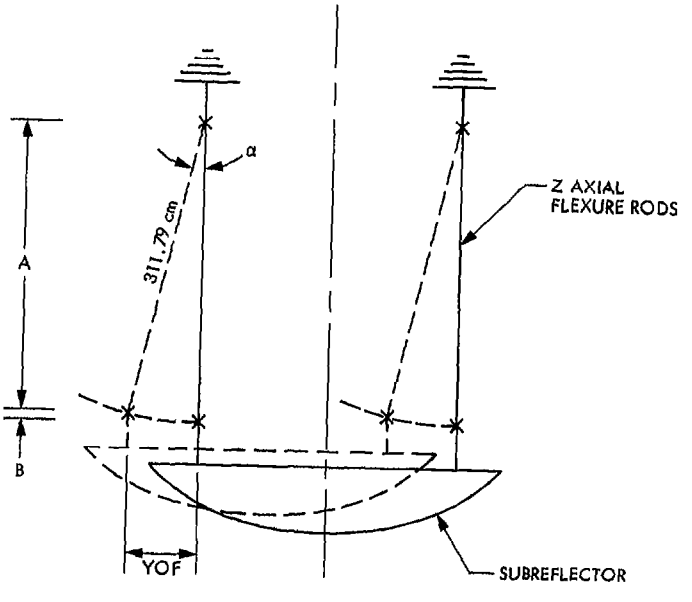

Fig. 5. The 64-m subreflector axial-Z defocus resulting from lateral-Y motion or offset

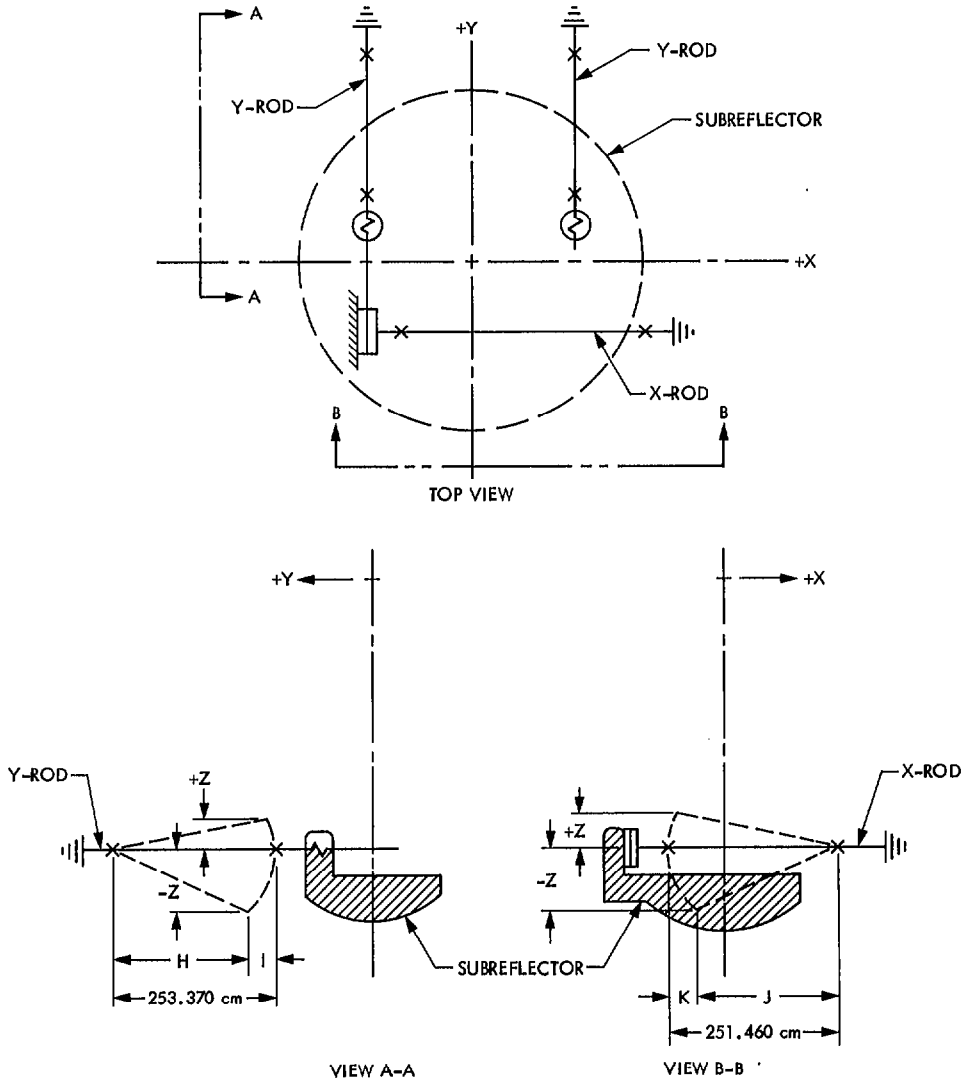

Fig. 6. The 64-m subreflector *X* and *Y* Support Rods. The *X* and *Y* lateral defocus is cross-coupled from axis-Z motion.

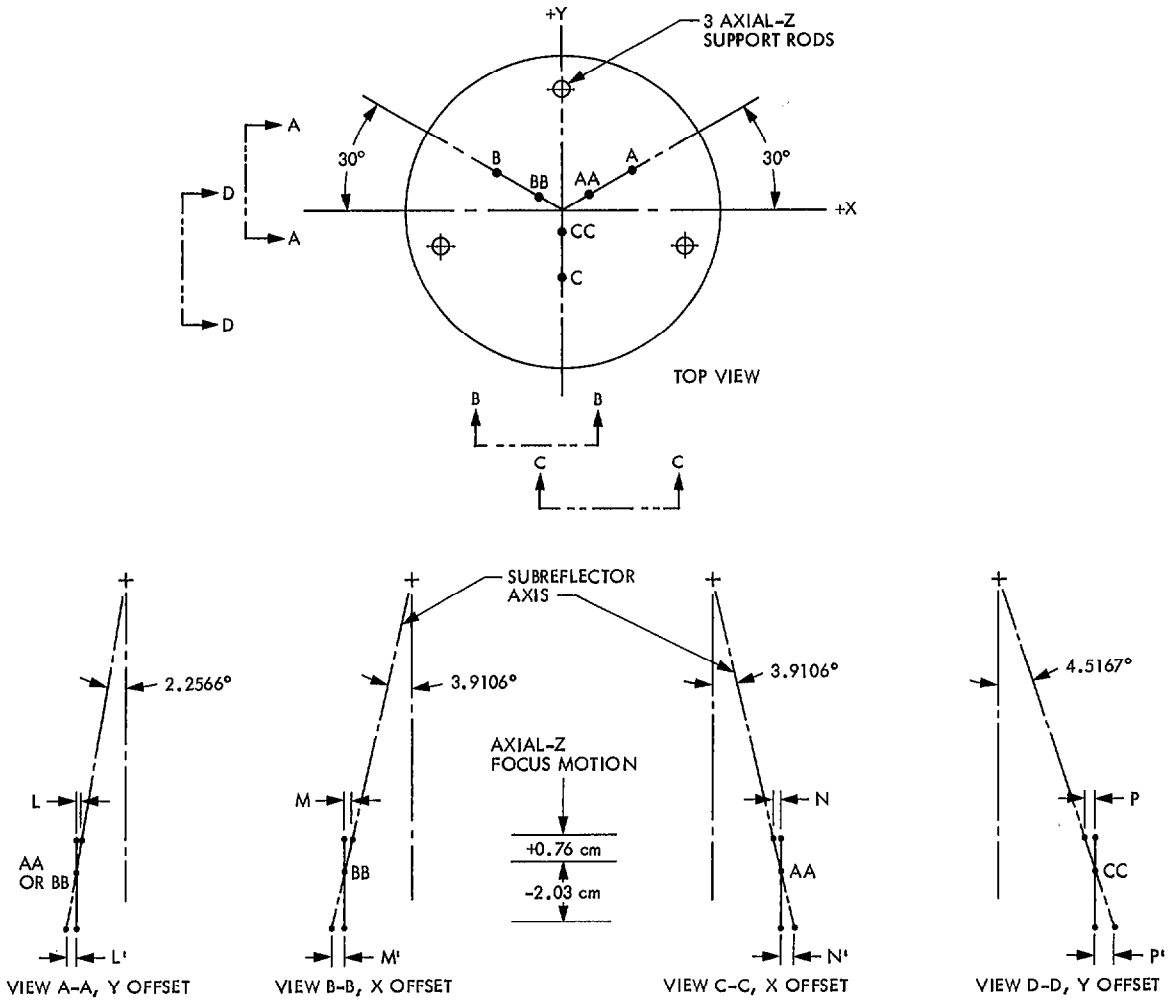

Fig. 7. The 64-m subreflector *X* and *Y* lateral offset from axial-*Z* focus motions

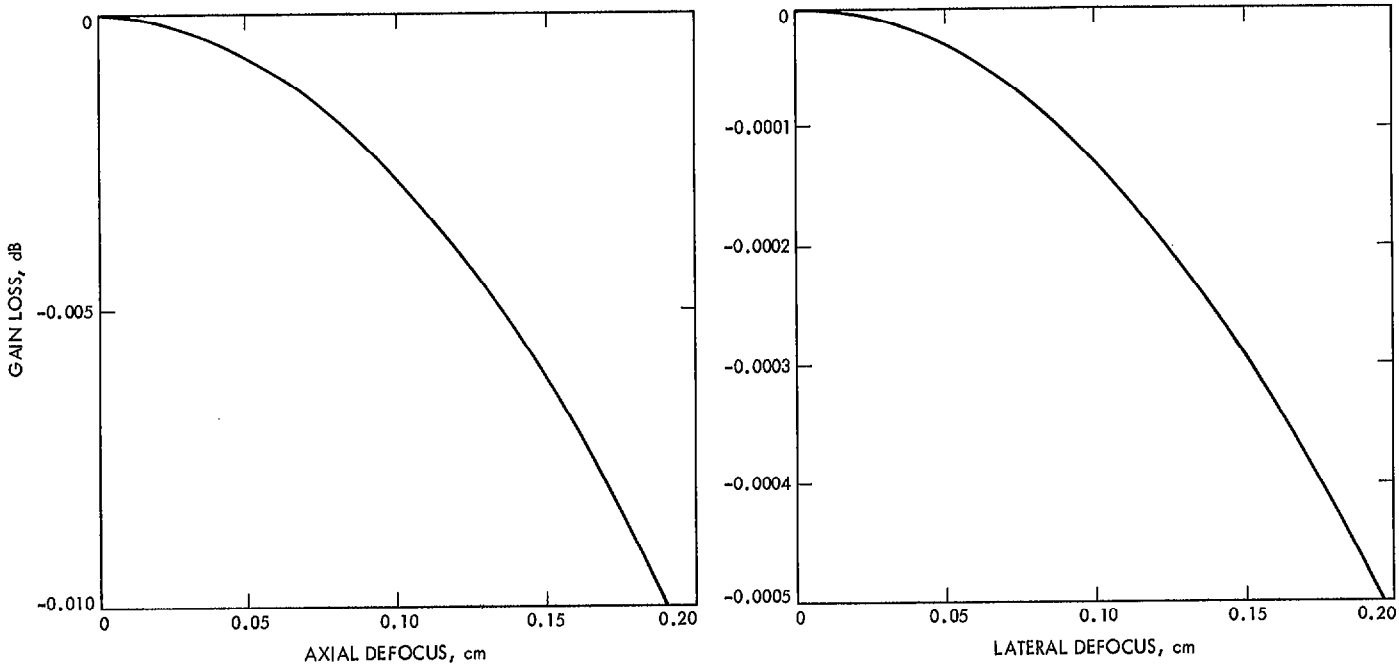

$$\text{GAIN LOSS, dB (RUZE)} = 10\ \text{LOG}_{10}\left(\exp\left[-16\,\pi^2\left(\frac{\text{RMS}}{\lambda}\right)^2\right]\right)$$

$$= 10\ \text{LOG}_{10}\left(\exp\left[-16\,\pi^2\left(\frac{\text{OFFSET-CM} \times \text{SLOPE} - \frac{\text{mm}}{\text{cm}}}{\lambda - \text{mm}}\right)^2\right]\right)$$

$$\left.\begin{aligned}\text{AXIAL OFFSET SLOPE} &= 0.7111\ \frac{\text{mm}}{\text{cm}}\\ \text{LATERAL OFFSET SLOPE} &= 0.1553\ \frac{\text{mm}}{\text{cm}}\end{aligned}\right\}\ \text{FOR F/D} = 0.4235$$

Fig. 8. The 64-m antenna (F/D = 0.4235) gain loss vs axial and lateral defocus

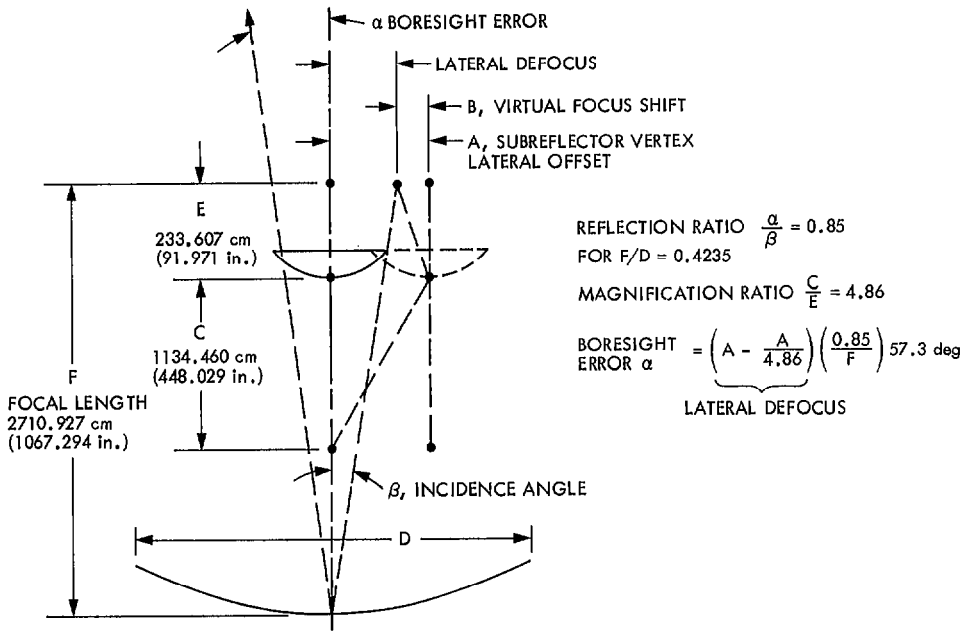

Fig. 9. The 64-m antenna boresight error from subreflector lateral shift

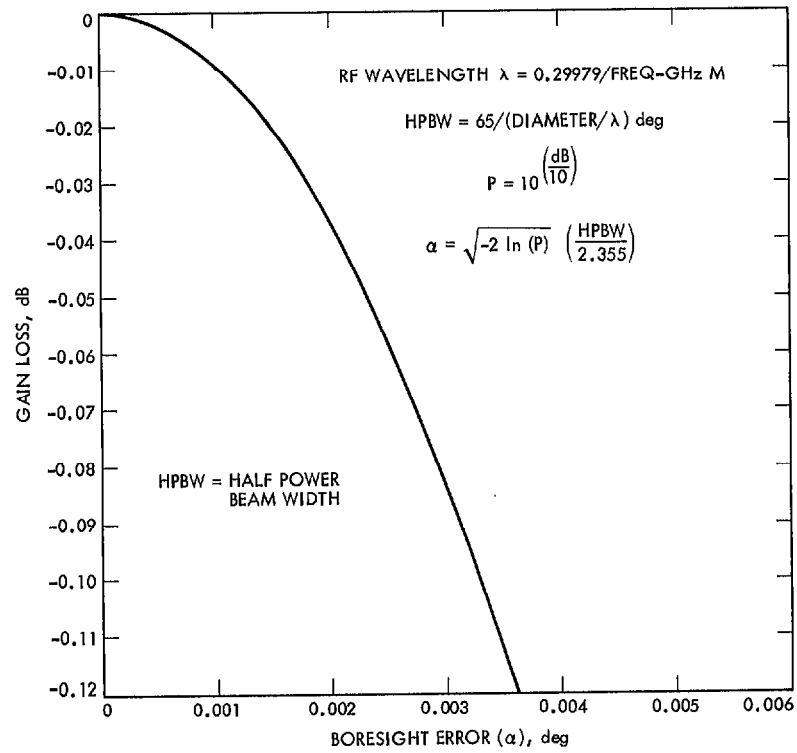

Fig. 10. The 64-m antenna gain loss vs boresight errors. Uniform amplitude illumination assumed.